FEBS Letters 587 (2013) 3522–3528

FEBS Letters

journal homepage: www.FEBSLetters.org

NMR structure and MD simulations of the AAA protease intermembrane space domain indicates peripheral membrane localization within the hexaoligomer

Theresa A. Ramelot [a,*], Yunhuang Yang [a], Indra D. Sahu [a], Hsiau-Wei Lee [b], Rong Xiao [c,d], Gary A. Lorigan [a], Gaetano T. Montelione [c,d], Michael A. Kennedy [a,*]

[a] Department of Chemistry and Biochemistry, Northeast Structural Genomics Consortium, Miami University, Oxford, OH 45056, USA
[b] Complex Carbohydrate Research Center, Northeast Structural Genomics Consortium, University of Georgia, Athens, GA 30602, USA
[c] Center for Advanced Biotechnology and Medicine, Department of Molecular Biology and Biochemistry, Northeast Structural Genomics Consortium, Rutgers, University, Piscataway, NJ 08854, USA
[d] Department of Biochemistry, Robert Wood Johnson Medical School, Piscataway, NJ 08854, USA

ARTICLE INFO

Article history:
Received 16 July 2013
Revised 21 August 2013
Accepted 6 September 2013
Available online 18 September 2013

Edited by Maurice Montal

Keywords:
m-AAA protease
Molecular dynamics
NMR structure

ABSTRACT

We have determined the solution NMR structure of the intermembrane space domain (IMSD) of the human mitochondrial ATPase associated with various activities (AAA) protease known as AFG3-like protein 2 (AFG3L2). Our structural analysis and molecular dynamics results indicate that the IMSD is peripherally bound to the membrane surface. This is a modification to the location of the six IMSDs in a model of the full length yeast hexaoligomeric homolog of AFG3L2 determined at low resolution by electron cryomicroscopy [1]. The predicted protein–protein interaction surface, located on the side furthest from the membrane, may mediate binding to substrates as well as prohibitins.

1. Introduction

Here we report the solution NMR structure of the intermembrane space domain (IMSD, residues) of human mitochondrial ATPase associated with various activities (AAA) protease AFG3-like protein 2 (AFG3L2). In humans, AFG3L2 forms homo- or hetero-oligomeric complexes with paraplegin (49% identical) in the mitochondrial inner membrane (IM). They are named *m*-AAA proteases, meaning that their catalytic domains are located in the mitochondrial *m*atrix. The catalytic domains of both AFG3L2 and paraplegin are made up of two subunits, the ATPase associated AAA domain and the metallopeptidase domain (PD) responsible for substrate proteolysis. A single chain of AFG3L2 or paraplegin has two transmembrane (TM) helices, so that the topology in the IM results in the short N-terminus and large catalytic domain on the matrix side and a small ~70-residue IMSD on the lumen side. Established and putative functions for *m*-AAA proteases have been extensively characterized and several recent reviews are available [2–4]. Although the crucial functions of *m*-AAA proteases are proteolytic processing and degradation of both non-membrane and membrane-embedded substrates, the role of IMSDs remains to be determined.

AFG3L2 and paraplegin have mammalian, plant, and fungal homologs, including yeast Yta10 and Yta12 (59% identical to AFG3L2) in addition to the well-studied bacterial homolog, FtsH (filamentous temperature sensitive H, 45% sequence identity), which forms only homo-oligomers, and is essential for survival in *Escherichia coli*. The IMSD of AFG3L2 belongs to a conserved protein family (Pfam), Pfam PF06480.

Prior to the NMR structure reported here, no atomic resolution information was available for domains in this diverse Pfam. However, the overall architecture of a *m*-AAA protease was recently determined in a 12 Å-resolution cryo-electron tomography (CET) map of yeast Yta10/Yta12 hetero-oligomer solubilized in a detergent micelle [1]. The authors observed symmetrical hexamers that rely on residues in PD for oligomerization. In their model, the six IMSDs splayed-out in a hexagon around 12 clustered TM helices and have no contact with IMSDs on other subunits [1]. Prediction of the IM position based on the location of the TM helices resulted in the IMSDs being half buried in the membrane. Our results, however, are inconsistent with this aspect of the model, rather, our data suggests that this domain has only peripheral contacts with

* Corresponding authors. Fax: +1 513 529 5715.
E-mail addresses: theresa.ramelot@miamiOH.edu (T.A. Ramelot), kennedm4@miamiOH.edu (M.A. Kennedy).

0014-5793/$36.00 © 2013 Published by Elsevier B.V. on behalf of the Federation of European Biochemical Societies.
http://dx.doi.org/10.1016/j.febslet.2013.09.009

the IM. We propose a modification to the previous model that is consistent with our structural data and molecular dynamics (MD) simulations.

2. Materials and methods

2.1. Cloning, expression and purification

The selected IMSD fragment of the *afg3l2* gene was cloned into a pET15 expression vector (NESG Clone ID HR6741A-15.1) as described elsewhere [5,6]. The IMSD, residues 164–251 of AFG3L2, included 11 non-native N-terminal residues (MGHHHHHHSHM). Expression and purification were conducted following standard protocols of the Northeast Structural Genomics Consortium (NESG) to prepare [U-^{13}C, ^{15}N]- and U-^{15}N, 5% biosynthetically-directed ^{13}C (NC5) samples [5,6] and details can be found in Supplemental Procedures. The final NMR samples were 0.7–1.0 mM in the NMR buffer: 20 mM MES, 100 mM NaCl, 5 mM $CaCl_2$, 10 mM dithiothreitol, and 0.02% NaN_3 at pH 6.5. The protein was monomeric under the conditions used in the NMR experiments based on analytical static light scattering in-line with gel filtration chromatography and rotational correlation time estimates from ^{15}N relaxation data (τ_c 7.1 ± 0.5 ns, Fig. S1).

2.2. NMR and structure determination

NMR data were collected at 298 K on NC and NC5 samples of ~300 μl in 5 mm Shigemi NMR tubes on 600 MHz Varian Inova spectrometer with a 5-mm HCN cold probe and 850 MHz Bruker Avance III spectrometer equipped with a conventional 5-mm HCN probe. A description of NMR experiments and methods for structure determination and refinement can be found in Supplemental Procedures. The assigned ^{1}H–^{15}N HSQC spectrum is provided as Fig. S2. Chemical shifts, NOESY peak lists, and raw FIDS were deposited in the BioMagResBank with ID 18156). The final ensemble of 20 models and NMR resonance assignments were deposited to the Protein Data Bank with ID 2LNA.

2.3. MD simulations

MD studies of the lowest energy structure from the NMR ensemble (residues 16–95) with a 1-palmitoyl-2-oleoylphosphatidylcholine (POPC) membrane were performed using NAMD version 2.9 [7] with the CHARMM27 [8] force field. The Visual Molecular Dynamics software, VMD version 1.8.7 [9], was used for simulation setup and MD trajectory analysis. A pre-equilibrated POPC bilayer with an 80 Å^2 surface was generated with the VMD membrane builder plugin. The IMSD was positioned >8 Å above the membrane and the system was solvated into a water box and neutralized with NaCl. Equilibration and simulations were performed similar to those reported in the KcsA tutorial for VMD and NAMD [10] and is described in detail in the Supplemental Procedures.

3. Results

3.1. Solution NMR structure

The human AFG3L2 IMSD features an uncommon mixed α + β fold comprised of two α-helices (α1, 20–30; α2, 67–81) and a five-stranded β-sheet (β1, 16–17; β2, 33–39; β3, 43–48; β4, 60–63; β5, 91–93;) arranged in a βαββββαβ topology (Fig. 1A–C). The first helix (α1) has a break at Tyr27 resulting in a bend in the helix. The β-sheet has an up–up–down–up–up topology with the order β1–β4–β3–β2–β5 and packs against the two helices to form a compact structure, whereas a poorly-defined loop is located between β3 and β4 (loop 3–4; Thr49-Gln58). Structural statistics for the NMR ensemble are presented in Supplemental Table S1.

3.2. Homologs have the same predicted secondary structure

IMSDs of human paraplegin, yeast Yta10 and Yta12, share 36%, 40%, and 43% sequence identity with that of human AFG3L2. However, these ~85-residue domains were all predicted to have the same order of secondary structural elements by PSIPRED 3.0 [11] (Fig. 1D). The prediction for the human AFG3L2 IMSD was in good agreement with the NMR structure with the exception that the first short β-strand was slightly shifted from the PSIPRED prediction (Fig. 1D). Similarly, the ~70-residue *E. coli* FtsH periplasmic domain had an equivalent secondary structure prediction although it is ~14 residues shorter (Fig. 1D). This result suggests that the IMSD structure will be conserved within Pfam PF06480, including bacterial homologs.

3.3. Structural alignment comparison and protein–protein interaction prediction

Structural alignment analysis of AFG3L2 IMSD by Dali [12] found no protein structures with RMSD <2.5 Å or sequences with >20% identity. Dali identified the 60S eukaryotic ribosome subunit protein L38 (PDB ID 3U5E:k and 4A18:p, Z-scores 4–5) as a similar topology protein. L38 is part of a large complex of ribosomal proteins. According to predictions of protein–protein interactions by PredUS [13], residues near α1 (Asn 26) and part of the α2-loop-β5 (Gly82-Glu86, with the highest score for Gly85) are likely to interact with other proteins (Fig. 3C and D). The prediction is primarily due to structural alignment with the N-terminal domain of the molecular chaperone heat shock protein Hsp90 (Fig. S4). This domain contains an ATP binding site and binds co-chaperones (reviewed in [14]). In human cells, Hsp90 binds to more than 10 known co-chaperones that together with Hsp90 regulate the stability and activation of other proteins, many of which are involved in cellular signaling pathways. For example, the co-chaperone Cdc37 regulates Hsp90 interactions with kinases and the stability of the respective kinases determined the extent of association with Hsp90, with unstable kinases having increased affinity [15]. Taken together, the structural alignment results indicate a role in the assembly of protein–protein complexes that could regulate substrate recognition.

3.4. Membrane interaction surface

In AFG3L2, the interaction of the IMSD with the membrane is governed, in part, by the tethering to the TM helices at its N- and C-termini. Analysis of the IMSD surface electrostatic surface potential [16] revealed a patch of basic and hydrophobic residues at one end of the protein that constitutes a putative membrane interaction surface (Fig. 2A–D). It is primarily made up of loops between secondary structural elements, including loop 2–3 and loop 3–4 (Fig. 2A–D). Solvent exposed hydrophobic residues, as well as basic residues from this surface are shown in Fig. 2A and B. It is well known that Trp and Tyr residues have a preferred localization at membrane interfaces and that Arg and Lys residues can interact with phospholipid headgroups.

ConSurf [17] analysis revealed that conserved residues across the eukaryotic homologs are located on one side and that the putative membrane binding surface has few conserved residues. The conserved surface patch has an acidic surface resulting primarily from residues Glu71 and Glu75 (Fig. 2C and E), but the function of this patch is unknown. On the putative membrane-binding

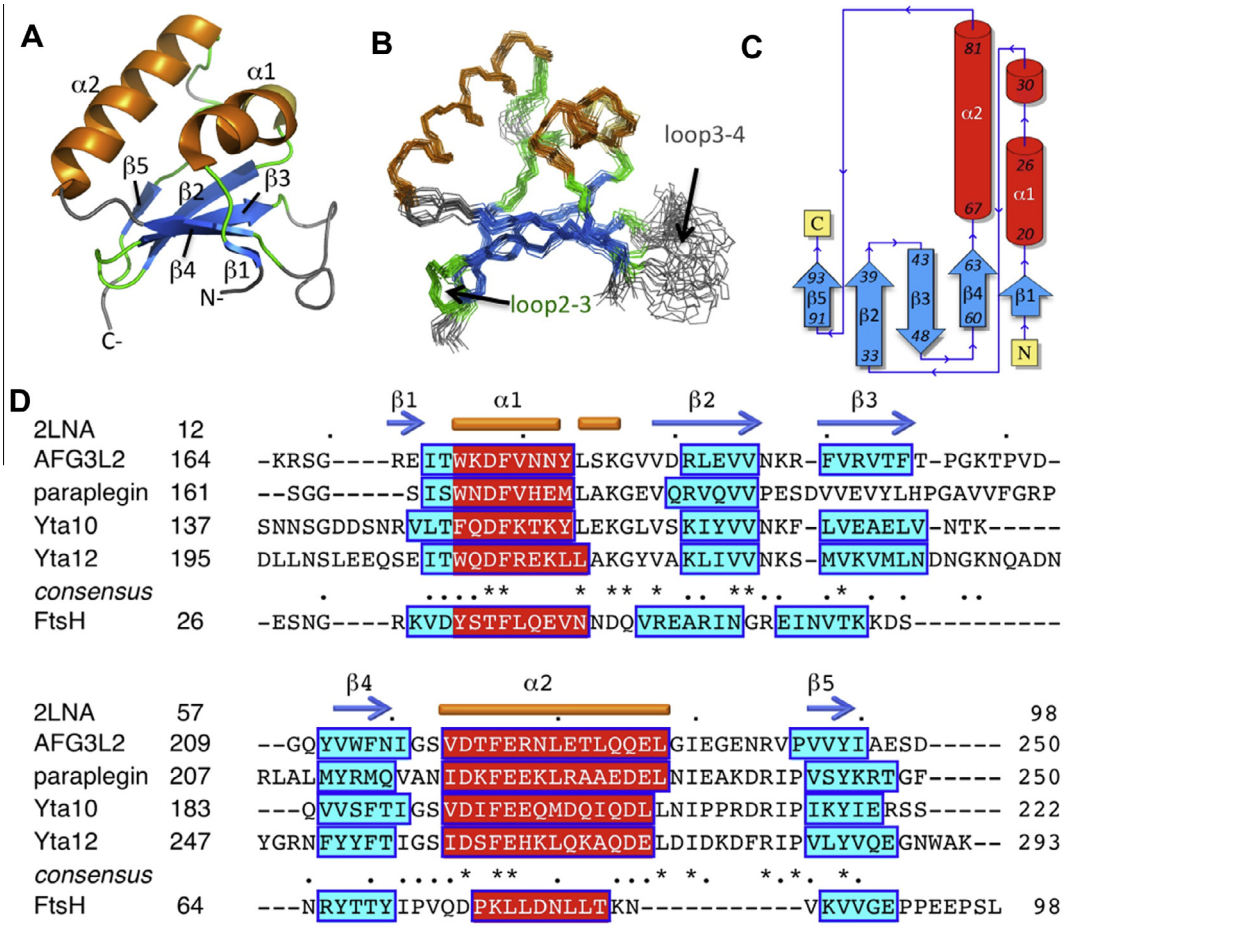

Fig. 1. Structure and topology of AFG3L2 IMSD. (A) Cartoon representation of the lowest energy NMR structure, α-helices and β-strands are shown in blue and orange, and loops are colored green or grey, if they were not ordered residues. (B) Superposition of the final ensemble of 20 models (residues 14–96). (C) Domain topology obtained using PDBSum [35]. (D) IMSDs from human AFG3L2 and paraplegin, yeast Yta10 and Yta12, and *E. coli* FtsH. Alignment of human and yeast sequences was performed with Clustal W 2.0 [36] and the consensus is reported. FtsH alignment is based on secondary structure prediction by PSIPRED 3.0 [11]. Secondary structure for the NMR structure of human AFG3L2 IMSD, PDB ID 2LNA, is shown above the sequences.

surface, only a few residues are conserved (Lys41 and G65), and loop 3–4 is variable among the sequence homologs (Fig. 2F).

3.5. MD simulations of IMSD and POPC membrane

In order to elucidate the specific membrane interactions and orientation of the IMSD relative to the mitochondrial IM, extensive all-atom MD simulations were carried out. A lipid bilayer membrane of POPC was chosen since phosphatidylcholines are the most abundant phospholipids in the mitochondrial IM (~38% overall) [18]. All-atom simulations of peripheral protein–membrane interactions have been used to determine the extent of the interactions and are typically performed for tens to thousands of ns (several are reviewed in [19,20]). During the MD simulation, the IMSD spontaneously approached and interacted with the membrane within 40 ns. We ran the MD trajectory for 200 ns, in three independent computations, until the protein orientation with respect to the membrane appeared to converge.

At the end of the three MD trajectories, IMSD orientations were in agreement with our proposed membrane interaction surface based on the surface charge distribution (Fig. 2D). The C-terminal end of α2 was positioned furthest from the POPC membrane patch (Gly85 immediately follows this helix) (Fig. 3A). The Trp61 side chain was near, or embedded in, the membrane at the end of each simulation (Fig. 3A). Lys41 in loop 2–3 was close enough to interact with the phosphate moiety of the lipids at certain times in the MD simulations. Near the end of the MD trajectories, loop 3–4 (Gly57), and both N- and C-termini were within 10 Å of the membrane surface, demonstrating that these regions of the IMSD can simultaneously interact with the membrane (Fig. 3B and C). In only the second MD run, loop 3–4 formed a helix at 50 ns and remained helical for the rest of the simulation (Fig. 3C), indicating that this loop has helical propensity when in proximity to the membrane. The results from all three MD runs are provided in Fig. S3.

3.6. Model for full-length AFG3L2

Since experimental characterization of the membrane interaction has not been successful, our membrane interaction model of the IMSD is based on the solution structure of the domain and MD simulation results. Titration of the NMR sample with dodecyl phosphocholine micelles resulted in complete unfolding of the protein and addition of POPC liposomes resulted in no change in the ^{1}H–^{15}N HSQC spectrum (data not shown), although disappearance of NH peak intensities would be expected of the IMSD was in slow exchange with the liposomes. These results further suggest that this water-soluble domain is not likely to be half-buried in the mitochondrial membrane.

The IMSD structure is consistent with the shape of the domain obtained from the CET map of the Yta10/Yta12 hexaoligomer solubilized in *n*-octyl-β-D-glucopyranoside (β-OG) detergent micelles

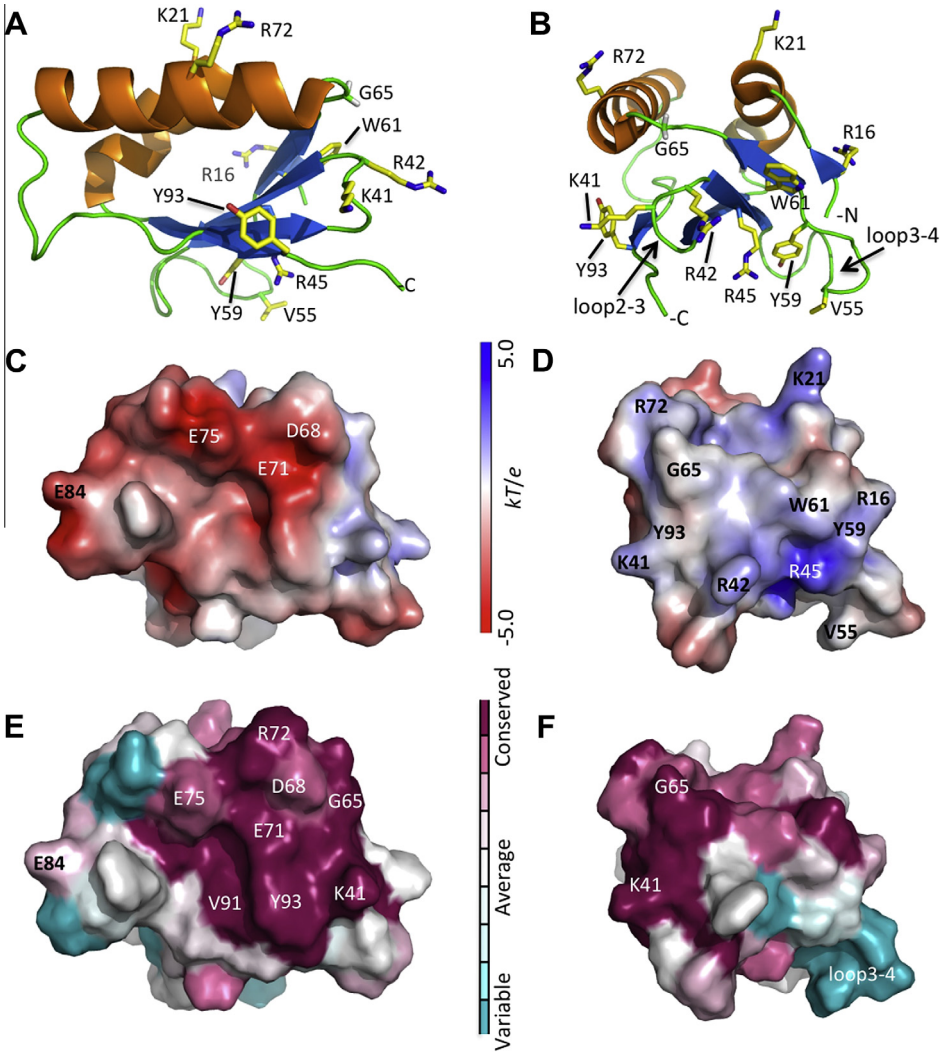

Fig. 2. Structure and membrane interaction surface of IMSD (A) Solution NMR structure of the human IMSD from AFG3L2 (residues 14–96), selected side chains are shown. (B) Cartoon figure rotated from A to show the proposed membrane interaction residues. (C and D) APBS [16] solvent accessible electrostatic surface potential with same orientation as in A and B showing negative (red), neutral (white), and positive (blue) charges. (E and F) ConSurf [17] image showing the conserved surface residues. Residue coloring reflects the degree of residue conservation for selected eukaryotic homologs from Pfam06480 (42 sequences). All figures were rendered using PyMOL (DeLano Scientific).

(Fig. 4A and B). Modeling of the IM based on the location of the 12 TM helices resulted in the IMSDs being approximately half-buried in the membrane (Fig. 4B). As noted by the authors, the cryo-EM structure determined in a micelle environment may differ from the native structure in the mitochondrial IM [1]. Indeed, since the β-OG micelles have a radius of gyration of ~30 Å [21], the micelle surface surrounding the TM helices has sharp curvature compared to an membrane bilayer, and this could influence the position of IMSDs relative to the TM helices. In our new model, the IMSDs are reorganized so that they are positioned at the surface of the membrane (Fig. 4C). According to UniProt predictions [22] of the TM helix sequences (UniProt ID Q9Y4W6), there is a 4–5 residue "spacer" on either side of the domain (Arg16-Tyr93) to connect to the respective TM helices. Although the structure of this linker is unknown, this length appears sufficient to allow the required movement of the IMSDs. Also, the IMSDs may be situated closer together as well as above the membrane in the structure of the *m*-AAA protease in its native membrane (not shown in model).

4. Discussion

4.1. Prohibitin interactions with IMSDs

The *m*-AAA proteases have many experimentally determined protein substrates (reviewed in [2–4]). However, the only confirmed interaction partner for an IMSD is between the *E. coli* FtsH periplasmic domain and the HflK and HflC membrane protein complex (HflKC) [23], where HflK and HflC are related to eukaryotic prohibitin 1 (Phb1) and prohibitin 2 (Phb2). Prohibitins have a short hydrophobic stretch at their N-termini that anchors them to the membrane and the remaining ~30 kDa resides in the intermembrane space. This region of prohibitin consists of a so-called prohibitin (PHB) and a predicted coiled-coil (CC) segment at the C-terminal end [24]. Purified prohibitin complexes from yeast assumed large ~1 MDa ring-shaped structures with a diameter of ~20–27 nm containing equal amounts of Phb1 and Phb2 subunits by single particle electron microscopy [25]. The CC segment was required for assembly of the prohibitin complex [25]. However, it

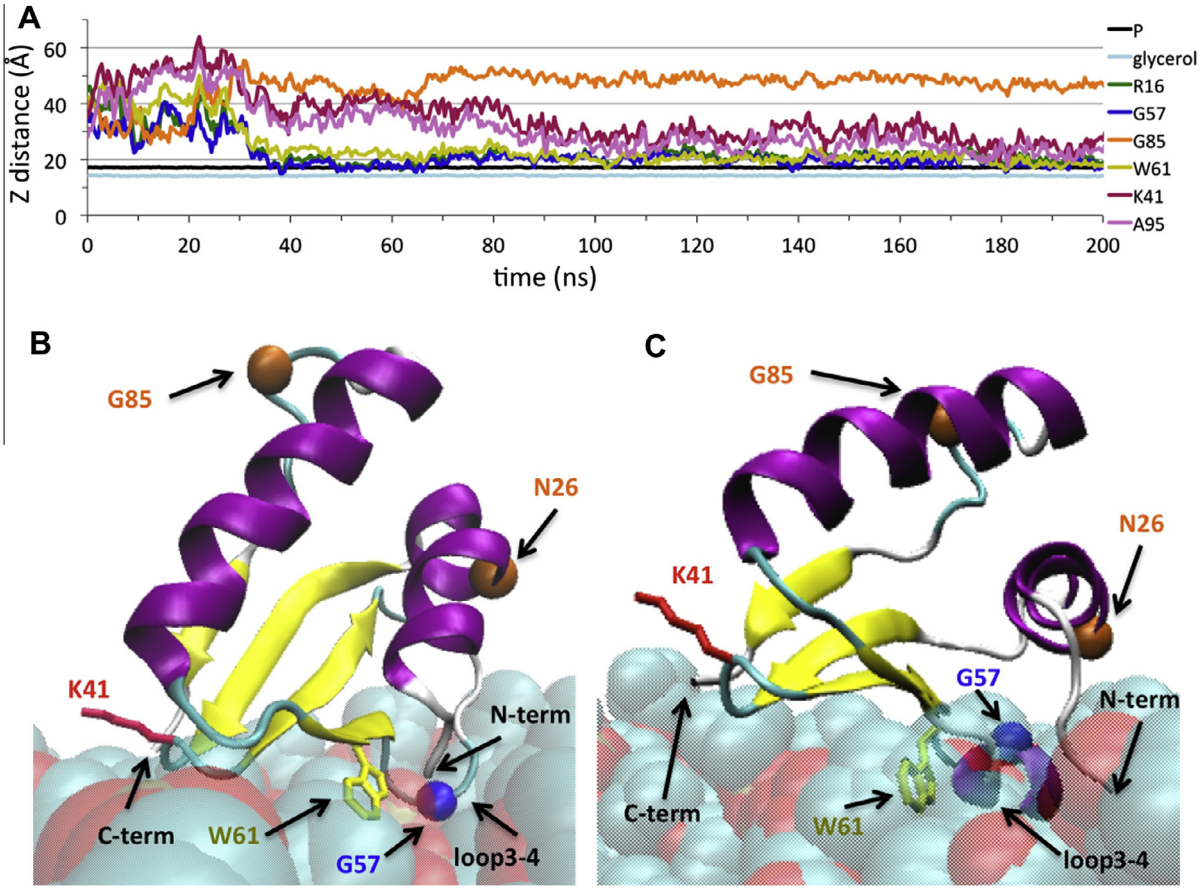

Fig. 3. (A) MD simulations of IMSD and POPC membrane. To characterize the extent of membrane insertion, the distance in the Z-dimension from the center of mass of the lipid atoms to selected lipid or protein atoms was calculated as a function of simulation time. Select protein atoms used for the analysis were the Arg16 (atom N) and A95 (atom C) to represent the N- and C-termini, respectively, Lys41 side chain (atom NZ) to represent loop 2–3, Gly57 (atom CA) to represent loop 3–4, Trp61 side chain (atom CZ2), and Gly85 (atom CA). Lipid atoms used were glycerol backbone (atoms C1–C3) and phosphates (atom P1). (B) and (C) Cartoon representation at 200 ns from the first and second MD simulation trajectories. The residues and atoms depicted in (A) are indicated as well as Asn26 and Gly85, shown with orange circles, that are predicted by PredUS [13] to have a highly propensity for protein–protein interactions. Figures were generated using VMD software and scripts [9].

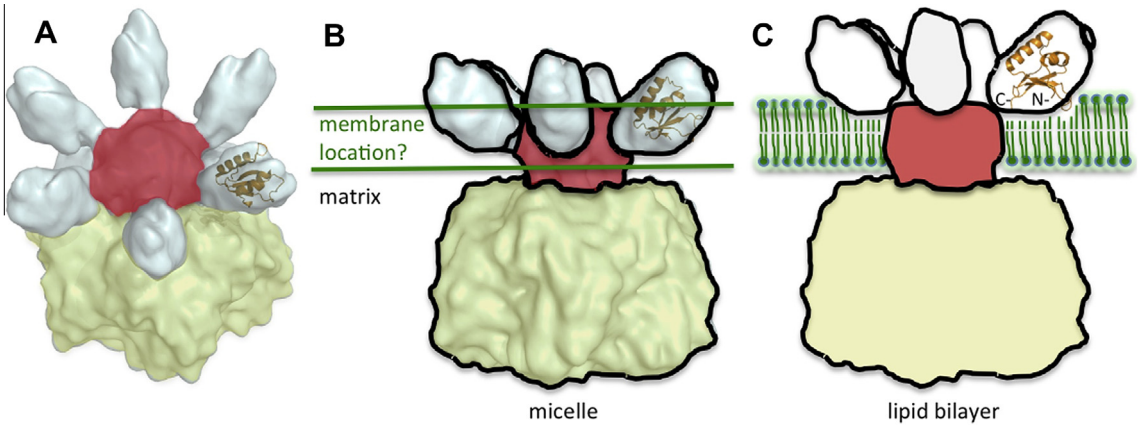

Fig. 4. Model of AFG3L2. (A) Cryo-EM structure of the yeast *m*-AAA protease with the human AFG3L2 shown as an orange cartoon manually fit into the density. The cryo-EM data was obtained from EMDataBank (ID 1712) [1], and PyMOL was used to generate the image. The matrix located AAA and PD domains are colored yellow, TM helices are colored red, and IMSDs are in white. (B) The membrane, depicted as green lines, is drawn based on the location of the TM helices in the detergent micelle. (C) Model of *m*-AAA protease in a lipid bilayer. The six IMSDs are positioned above the membrane, depicted as green phospholipids. The IMSD cartoon is shown as predicted by MD simulations.

is not known if the CC segment and/or the PHB domain interact with IMSDs.

In human mitochondria, both homo-oligomers of AFG3L2 and hetero-oligomers of AFG3L2 and paraplegin were found in a ~900 kDa protein complex by gel filtration and Blue Native PAGE [26,27], significantly larger than the ~400–500 kDa expected for *m*-AAA hexaoligomers. These complexes contain prohibitins as was demonstrated in mouse mitochondria [27], and in yeast, where prohibitins were associated with Yta10 and Yta12 in high molecular weight complexes [28]. In *E. coli* a molecular composition of

$(FtsH)_6(HflKC)_6$ was proposed [29], a result that supports a 1:1 interaction with the IMSD and each pair of prohibitin proteins. The human $(AFG3L2)_6(Phb1–Phb2)_6$ complex would be 866 kDa, which is consistent with the experimentally determined molecular weight of the complex. This supports a complex with 12 copies of Phb1–Phb2 in a ring around the *m*-AAA protease; a structure that seems likely based on the spread-out sixfold positioning of IMSDs in the *m*-AAA hexaoligomer with a 13 nm diameter [1]. This would fit nicely inside the prohibitin central cavity of 9–16 nm [25]. It is also consistent with our model with the IMSD protein–protein interaction interface on the top, outside surface of the hexaoligomer and the membrane-interaction surface at the bottom (Fig. 4). However, it remains to be experimentally determined whether the protease will be inside or outside the prohibitin ring structure [24]. Estimations of the number of copies of Phb1–Phb2 in the yeast complex vary from 12–16 or 16–20 [25,30]; it should be noted that the ring complexes had variability in their shape and size [25].

The role of prohibitins and their interactions *m*-AAA proteases is not well understood. In yeast mitochondria, prohibitins may act as negative regulators of *m*-AAA proteolysis of non-assembled IM proteins or newly synthesized proteins because deletion of Phb1 or Phb2 results in accelerated proteolysis by the *m*-AAA protease [28,30]. Prohibitins could prevent accessibility of targets to *m*-AAAs by binding to the substrate or by changing the protease activity. A direct interaction between prohibitins and newly synthesized mitochondria proteins was demonstrated in yeast by co-immunoprecipitation indicating a role of prohibitins as chaperones that stabilize these proteins [30]. Furthermore, human Phb1 shares sequence similarity with the bacterial chaperone GroEL, called Hsp60 in eukaryotes [30]. It has also been suggested that prohibitins may act as a scaffold to maintain the correct organization of proteins in a lipid raft environment in order to physically separate the substrate from the protease [24,31]. Taken together, *m*-AAA proteases and prohibitins may play a role in stabilization of membrane protein complexes and other chaperone-like activities [2–4].

4.2. Possible role for IMSD in substrate recognition

In general, recognition involves substrate binding to the AAA domain, followed by ATP-dependent unfolding and translocation, and progressive proteolysis by the PD domain. However, substrate recognition by *m*-AAA proteases is not entirely understood. In *E. coli*, FtsH recognized membrane proteins with 10–20 residue unstructured N- or C-terminal ends [32]. Recognition may not have sequence specificity but rather seems to target a broad range of unstructured polypeptides [32]. These would include misfolded, damaged, or non-assembled subunits. In yeast mitochondria, deletion of the IMSD along with the two TM segments impaired proteolysis of integral membrane proteins, indicating a possible role for IMSDs in recognition of membrane proteins [33]. For proteins that have residues in the intermembrane space this role could be direct or indirect through interactions with adaptor/chaperone proteins.

Another complexity is that substrate recognition may be different for different targets. For example, deletion of the periplasmic domain in *E. coli* resulted in FtsH that could still degrade the membrane protein SecY but not the cytosolic protein CII [23]. This FtsH mutant could no longer bind to HflKC, suggesting that prohibitins can modulate interactions of some protein targets with the *m*-AAA protease. In addition to prohibitins, it is likely that other specific adaptors/chaperones interact with diverse *m*-AAA target proteins as is the case for other AAA proteases such as the prokaryotic Clp proteases [34]. Based on our data and current understanding of *m*-AAA function, we suggest that protein–protein interactions with IMSDs will modulate degradation of a subset of protein targets.

Acknowledgments

Grant sponsor National Institute of General Medical Sciences Protein Structure Initiative – Biology (PSI-Biology); Grant numbers: U54-GM094597 in support of the NESG (G.T.M. and M.K.) and U01-GM094622 in support of the Mitochondrial Protein Partnership (MPP) (John L. Markley, PI, and David J. Pagliarini, Co-PI). The target was nominated by the MPP, University of Wisconsin-Madison. The NAMD work was supported by computing time allocation from the Ohio Supercomputer Center (OSC), start-up project PMIU0117 to T.A.R.

We thank J. Mueller for assistance with parallelization of NAMD on the Miami University Redhawk Cluster and OSC. We thank Y.J. Huang and J.K. Everett for construct design, and H. Janua, E. Kohan, R. Shastry, and T. Acton at the Rutgers' protein production facility for technical support. Most NMR data collection was conducted at the Ohio Biomedicine Center of Excellence in Structural Biology and Metabonomics at Miami University.

Appendix A. Supplementary data

Supplementary data (four supplemental figures and methods) associated with this article can be found, in the online version, at http://dx.doi.org/10.1016/j.febslet.2013.09.009.

References

[1] Lee, S. et al. (2011) Electron cryomicroscopy structure of a membrane-anchored mitochondrial AAA protease. J. Biol. Chem. 286, 4404–4411.
[2] Janska, H., Kwasniak, M. and Szczepanowska, J. (2013) Protein quality control in organelles – AAA/FtsH story. Biochim. Biophys. Acta 1833, 381–387.
[3] Gerdes, F., Tatsuta, T. and Langer, T. (2012) Mitochondrial AAA proteases–towards a molecular understanding of membrane-bound proteolytic machines. Biochim. Biophys. Acta 1823, 49–55.
[4] Langklotz, S., Baumann, U. and Narberhaus, F. (2012) Structure and function of the bacterial AAA protease FtsH. Biochim. Biophys. Acta 1823, 40–48.
[5] Acton, T.B. et al. (2011) Preparation of protein samples for NMR structure, function, and small-molecule screening studies. Methods Enzymol. 493, 21–60.
[6] Xiao, R. et al. (2010) The high-throughput protein sample production platform of the Northeast Structural Genomics Consortium. J. Struct. Biol. 172, 21–33.
[7] Phillips, J.C. et al. (2005) Scalable molecular dynamics with NAMD. J. Comput. Chem. 26, 1781–1802.
[8] MacKerell Jr., A.D. et al. (1998) All-atom empirical potential for molecular modeling and dynamics studies of proteins. J. Phys. Chem. B 102, 3586–3616.
[9] Humphrey, W., Dalke, A. and Schulten, K. (1996) VMD: visual molecular dynamics. J. Mol. Graphics 14, 33–38.
[10] Aksimentiev, A., Sotomayor, M., Wells, D. http://www.ks.uiuc.edu/Training/Tutorials/science/membrane/mem-tutorial.pdf. (2012).
[11] Buchan, D.W.A. et al. (2010) Protein annotation and modelling servers at University College London. Nucleic Acids Res. 38, W563–568.
[12] Holm, L. and Rosenstrom, P. (2010) Dali server: conservation mapping in 3D. Nucleic Acids Res. (Suppl. 38), W545–W549.
[13] Zhang, Q.C. et al. (2011) PredUs: a web server for predicting protein interfaces using structural neighbors. Nucleic Acids Res. 39, W283–W287.
[14] Taipale, M., Jarosz, D.F. and Lindquist, S. (2010) HSP90 at the hub of protein homeostasis: emerging mechanistic insights. Nat. Rev. Mol. Cell Biol. 11, 515–528.
[15] Taipale, M. et al. (2012) Quantitative analysis of Hsp90-client interactions reveals principles of substrate recognition. Cell 150, 987–1001.
[16] Baker, N.A., Sept, D., Joseph, S., Holst, M.J. and McCammon, J.A. (2001) Electrostatics of nanosystems: application to microtubules and the ribosome. Proc. Natl. Acad. Sci. USA 98, 10037–10041.
[17] Ashkenazy, H., Erez, E., Martz, E., Pupko, T. and Ben-Tal, N. (2010) ConSurf 2010: calculating evolutionary conservation in sequence and structure of proteins and nucleic acids. Nucleic Acids Res. 38, W529–W533.
[18] Zinser, E. et al. (1991) Phospholipid synthesis and lipid composition of subcellular membranes in the unicellular eukaryote *Saccharomyces cerevisiae*. J. Bacteriol. 173, 2026–2034.
[19] Lindahl, E. and Sansom, M.S. (2008) Membrane proteins: molecular dynamics simulations. Curr. Opin. Struct. Biol. 18, 425–431.
[20] Stansfeld, P.J. and Sansom, M.S.P. (2011) Molecular simulation approaches to membrane proteins. Structure 19, 1562–1572.
[21] Lipfert, J., Columbus, L., Chu, V.B., Lesley, S.A. and Doniach, S. (2007) Size and shape of detergent micelles determined by small-angle X-ray scattering. J. Phys. Chem. B 111, 12427–12438.

[22] Apweiler, R. et al. (2012) Reorganizing the protein space at the Universal Protein Resource (UniProt). Nucleic Acids Res. 40, D71–75.
[23] Akiyama, Y., Kihara, A., Mori, H., Ogura, T. and Ito, K. (1998) Roles of the periplasmic domain of *Escherichia coli* FtsH (HflB) in protein interactions and activity modulation. J. Biol. Chem. 273, 22326–22333.
[24] Merkwirth, C. and Langer, T. (2009) Prohibitin function within mitochondria: essential roles for cell proliferation and cristae morphogenesis. Biochim. Biophys. Acta 1793, 27–32.
[25] Tatsuta, T., Model, K. and Langer, T. (2005) Formation of membrane-bound ring complexes by prohibitins in mitochondria. Mol. Biol. Cell 16, 248–259.
[26] Atorino, L. et al. (2003) Loss of *m*-AAA protease in mitochondria causes complex I deficiency and increased sensitivity to oxidative stress in hereditary spastic paraplegia. J. Cell Biol. 163, 777–787.
[27] Koppen, M., Metodiev, M.D., Casari, G., Rugarli, E.I. and Langer, T. (2007) Variable and tissue-specific subunit composition of mitochondrial *m*-AAA protease complexes linked to hereditary spastic paraplegia. Mol. Cell. Biol. 27, 758–767.
[28] Steglich, G., Neupert, W. and Langer, T. (1999) Prohibitins regulate membrane protein degradation by the *m*-AAA protease in mitochondria. Mol. Cell. Biol. 19, 3435–3442.
[29] Saikawa, N., Akiyama, Y. and Ito, K. (2004) FtsH exists as an exceptionally large complex containing HflKC in the plasma membrane of *Escherichia coli*. J. Struct. Biol. 146, 123–129.
[30] Nijtmans, L.G.J. et al. (2000) Prohibitins act as a membrane-bound chaperone for the stabilization of mitochondrial proteins. EMBO J. 19, 2444–2451.
[31] Merkwirth, C. et al. (2008) Prohibitins control cell proliferation and apoptosis by regulating OPA1-dependent cristae morphogenesis in mitochondria. Genes Dev. 22, 476–488.
[32] Chiba, S., Akiyama, Y. and Ito, K. (2002) Membrane protein degradation by FtsH can be initiated from either end. J. Bacteriol. 184, 4775–4782.
[33] Korbel, D., Wurth, S., Käser, M. and Langer, T. (2004) Membrane protein turnover by the *m*-AAA protease in mitochondria depends on the transmembrane domains of its subunits. EMBO Rep. 5, 698–703.
[34] Kirstein, J., Molière, N., Dougan, D.A. and Turgay, K. (2009) Adapting the machine: adaptor proteins for Hsp100/Clp and AAA+ proteases. Nat. Rev. Microbiol. 7, 589–599.
[35] Laskowski, R.A. (2009) PDBsum new things. Nucleic Acids Res. 37, D355–D359.
[36] Larkin, M.A. et al. (2007) Clustal W and Clustal X version 2.0. Bioinformatics 23, 2947–2948.